

Optical Engineering

SPIDigitalLibrary.org/oe

Long-term stability of Mg/SiC multilayers

Maria Guglielmina Pelizzo
Silvano Fineschi
Alain Jody Corso
Paola Zuppella
Piergiorgio Nicolosi
John Seely
Benjawan Kjornrattanawanich
David L. Windt

Long-term stability of Mg/SiC multilayers

Maria Guglielmina Pelizzo

CNR—Institute for Photonics and
Nanotechnologies LUXOR Lab.
via Trasea 7, 35131 Padova, Italy
and
University of Padova
Department of Information Engineering
via Gradenigo 6B, 35131 Padova, Italy
E-mail: pelizzo@dei.unipd.it

Silvano Fineschi

INAF—Osservatorio Astronomico di Torino
Via dell'Osservatorio, 20
I-10025 Pino Torinese (TO), Italy

Alain Jody Corso

Paola Zuppella

Piergiorgio Nicolosi

CNR—Institute for Photonics and
Nanotechnologies LUXOR Lab.
via Trasea 7, 35131 Padova, Italy
and
University of Padova
Department of Information Engineering
via Gradenigo 6B, 35131 Padova, Italy

John Seely

Space Science Division Naval Research
Laboratory
4555 Overlook Avenue S.W.
Washington, DC 20375

Benjawan Kjornrattanawanich

USRA and NSLS
Brookhaven National Laboratory
Upton, New York 11973

David L. Windt

Reflective X-ray Optics LLC
1361 Amsterdam Avenue
Suite 3B
New York, New York 10027

Abstract. Mg/SiC multilayers have been selected to coat the primary and secondary mirrors of the SCORE (Sounding-rocket CORonagraphic Experiment) telescope, a part of the NASA HERSCHEL program. Their experimental reflectance at the He II 30.4 nm wavelength is twice as much that of standard Mo/Si multilayer coatings, with a large improvement of the instrument effective area. Nevertheless, their long-term stability still needs to be evaluated in order to consider them as a valuable candidate for instrumentation of a long term space mission. A study is carried out on different Mg/SiC samples designed and fabricated varying the structural parameters and/or the capping layer material and thickness, which have been monitored for four years after deposition. © 2012 Society of Photo-Optical Instrumentation Engineers (SPIE). [DOI: 10.1117/1.OE.51.2.023801]

Subject terms: extreme ultraviolet; multilayer; space instruments; space applications; SiC/Mg; aging.

Paper 111305P received Oct. 20, 2011; revised manuscript received Dec. 27, 2011; accepted for publication Dec. 30, 2011; published online Mar. 7, 2012.

1 Introduction

Several space missions dedicated to the observation of the solar atmosphere and its surface dynamics have been planned by ESA and NASA. Among those missions, Solar Orbiter is an ESA Sun-observing satellite approved for launch in January 2017. The Multi Element Telescope for Imaging and Spectroscopy (METIS)¹ is a coronagraph of the Solar Orbiter payload,² characterized by a novel optical design,^{3,4} which will allow the imaging of the solar corona with unprecedented temporal and spatial resolution at different heights over the ecliptic plane. The current optical design of the METIS telescope is based on an on-axis Gregorian telescope with an external inverted occulter.

The telescope operates simultaneously in three spectral ranges: visible light between 450 and 650 nm and the two Lyman- α lines of hydrogen and helium, at H I 121.6 nm and He II 30.4 nm, respectively. In particular, the innovative coronagraph design foresees that each operational range shares a common optical path in the telescope (Fig. 1). The multiband capability of the telescope mirrors will be made possible by the use of multilayer coatings (MLs) deposited on the optical surfaces. Downstream of the telescope, a specially designed optical component, inserted in front of the focal plane, acts both as a mirror to deflect the visible light to the polarimeter assembly and as a filter to transmit the 121.6 nm light on to the focal plane. Alternatively, the insertion of an appropriate filter will allow imaging at 30.4 nm on the focal plane.

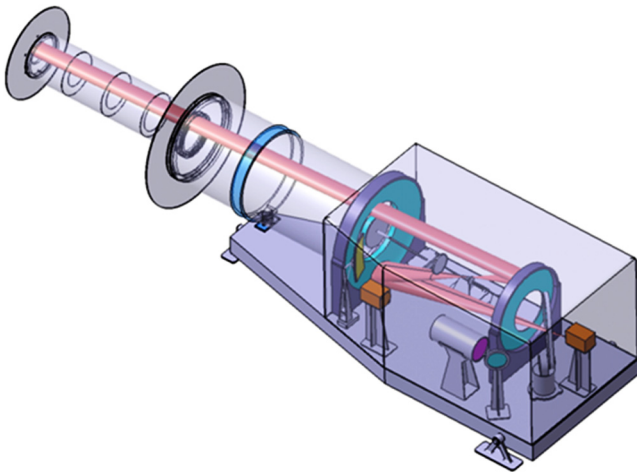


Fig. 1 METIS configuration layout.

Standard periodic Mo/Si ML coatings have been used in different space instruments.^{5,6} At 30.4 nm, they have a peak reflectance of only around 20%. That characteristic would strongly affect the performance of the METIS telescope in terms of effective area when observing in the Extreme Ultraviolet (EUV) range. The performance of such coatings could be improved either by controlling diffusion at interfaces⁷ or introducing gas incorporation on the Si spacer layers in order to reduce their density and consequently the absorption occurred in each bi-layer; the diminishing of the density of the spacer produces an increase of the contrast in reflection observed between Mo and Si during deposition, finally resulting in an enhancement of the Fresnel reflection coefficients at each interface.⁸ A peak reflectance improvement up to 26% can be achieved by the use of appropriate capping layer material,⁹ specially optimized using a technique already developed for lithography applications.^{10,11}

Structures based on different bilayer materials can reach higher efficiency than standard Mo/Si. In particular, Ir/Si ML was shown to provide reflectance up to 24% at 30.4 nm,¹² and Mo/Al/SiC ML up to 30%.¹³ The highest reflectance is, however, provided by the Mg/SiC ML, which was proposed for the atmospheric imaging assembly aboard the Solar Dynamics Observatory.¹⁴ This coating exhibits almost twice the peak reflectance of a standard Mo/Si coating, with an efficiency at 30.4 nm around 40%. For this reason, the Mg/SiC material combination has been studied by different research groups,^{15,16} which have demonstrated the thermal stability of the coating at high temperature. However, its stability over time still needs to be proven in order to validate such a coating for a long-lived space mission such as Solar Orbiter. In addition, the aging of such coatings, exposed to the laboratory atmosphere during the instrument fabrication and integration before launch, needs to be investigated. Furthermore, the MLs that will be used for the METIS mirrors also need to be tested in term of efficiency and long-term stability at 121.6 nm and in the visible spectral range, since they are intended to perform as multiband coatings.¹⁷

To prove the METIS innovative design concept, NASA has recently launched the instrument SCORE (Sounding-rocket CORonagraphic Experiment, Fig. 2)¹⁸ as part of the HERSCHEL program. SCORE represents a prototype of METIS. The sounding rocket was launched from the

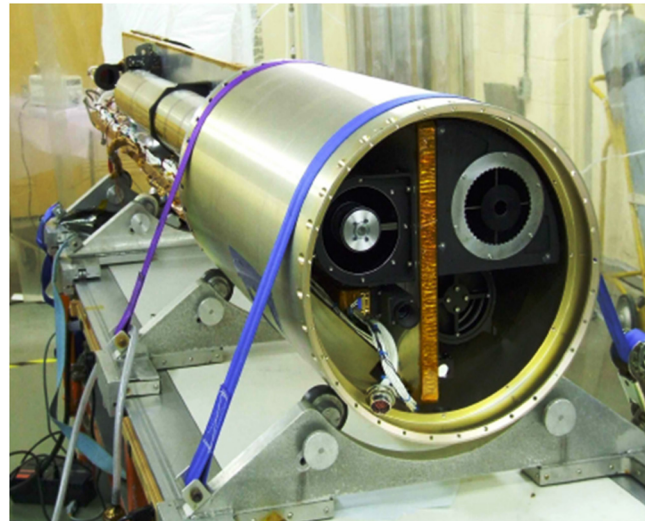


Fig. 2 SCORE sounding rocket before launch.

White Sands Missile Range in New Mexico on 14 September 2010, and the flight lasted a few minutes. Images of the solar corona at 30.4 nm and at 121.6 nm were acquired successfully.

In the case of SCORE, Mg/SiC MLs were selected to coat both the primary and secondary mirrors. Such coatings were optimized for the three spectral bands (Visible, UV, and EUV) by designing and developing Mg/SiC samples characterized by different structural parameters and capping layers. The selection of the most appropriate coatings for the SCORE mirrors was driven by the efficiency properties of these samples.

In this paper, we present the results of the characterization and comparison of Mg/SiC ML samples in two cases: just after the multilayer deposition and four years after deposition, in order to verify coating stability over time in laboratory conditions. The analyzed samples appear to have different levels of performance degradation, which are associated with different structural parameters.

2 Samples Design and Preparation

The different Mg/SiC samples have been designed by varying the structural parameters and/or the capping layer material and thickness. The sample A06012 must be considered as the baseline design, since it is a pure periodic structure optimized for peak reflectance at 30.4 nm. The structural parameters of this coating are reported in Table 1, where d is the period, Γ is the thickness ratio (thickness of

Table 1 Reference Mg/SiC ML parameters.

ML A06012	
d	15.64 nm
Γ	0.26
SiC	4.07 nm
Mg	11.57 nm
N	50

Table 2 Varied parameters for the different ML samples realized.

CODE	Gamma (Γ)	CODE	SiC top (nm)	CODE	Si top (nm)
A06012	0.26	A06012	0	A06012	0
A06011	0.22	A06016	1.5	A06021	1.5
A06013	0.30	A06015	3.0	A06022	3.0
A06014	0.19	A06017	4.5	A06023	4.5
		A06018	6.0	A06024	6.0
				A06025	9.0
				A06026	12.0

the absorber divided by the period d), and N is the number of periods. Other designs have been obtained by varying either Γ or the thickness of the SiC uppermost layer by depositing an additional layer of the same material (named hereafter SiC top), or alternatively by adding a Si top layer, as reported in Table 2.

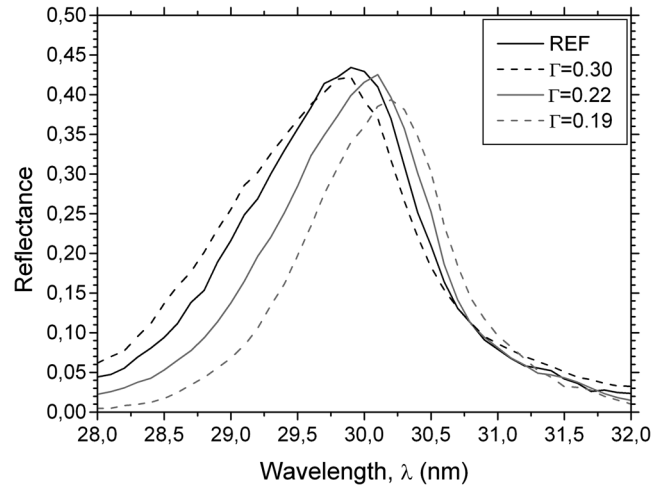


Fig. 3 Reflectance of the different samples obtained by varying Γ with respect to the Γ value of the A06012 reference sample.

The multilayer structures were deposited at RXO LLC (New York, USA) by DC magnetron sputtering on to polished Si(100) substrates of 16 mm \times 16 mm, using the system that was described by Windt and W.K. Waskiewicz.¹⁹

Table 3 Multilayer parameters obtained from the best fit of the reflectance data.

Sample	Γ	d	$\sigma_{\text{SiC-Mg}}$	$\sigma_{\text{Mg-SiC}}$	SiC Cap	Si Cap
A06011	0.27	15.61	1.59	2.33	SiO ₂ (0.18 nm)	
A06012	0.308	15.58	1.11	2.48	SiO ₂ (0.24 nm)	
A06013	0.372	15.63	1.49	2.20	SiO ₂ (0.22 nm)	
A06014	0.230	15.64	1.51	2.43	SiO ₂ (0.25 nm)	
A06015	0.325	15.63	1.53	2.59	SiO ₂ (0.23 nm) a-SiC(2.85 nm)	
A06016	0.325	15.58	1.45	2.55	SiO ₂ (0.20 nm) a-SiC(1.20 nm)	
A06017	0.323	15.56	1.51	2.55	SiO ₂ (0.26 nm) a-SiC(4.20 nm)	
A06018	0.320	15.55	1.60	2.49	SiO ₂ (0.24 nm) a-SiC(5.32 nm)	
A06021	0.322	15.54	1.42	2.41		SiO ₂ (0.61 nm) Si(0.82 nm)
A06022	0.310	15.50	1.40	2.40		SiO ₂ (0.58 nm) Si(2.33 nm)
A06023	0.315	15.49	1.44	2.46		SiO ₂ (0.60 nm) Si(3.61 nm)
A06024	0.314	15.49	1.43	2.41		SiO ₂ (0.57 nm) Si(5.59 nm)
A06025	0.315	15.34	1.38	2.30		SiO ₂ (0.65 nm) Si(8.10 nm)
A06026	0.321	15.47	1.45	2.37		SiO ₂ (0.71 nm) Si(11.12 nm)

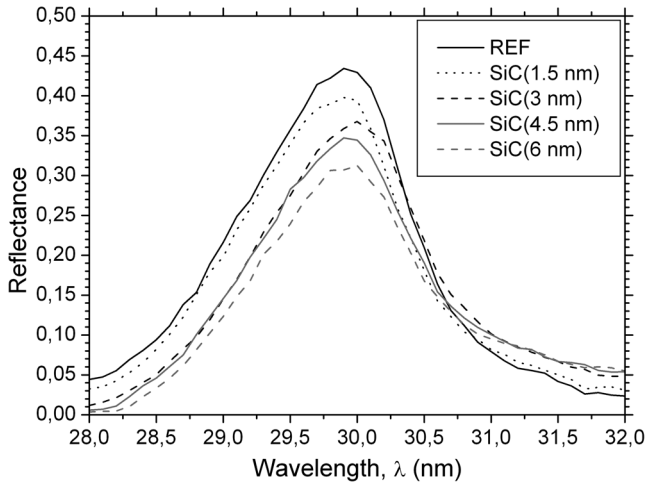


Fig. 4 Reflectance of the samples with additional SiC top layer and same structure as the A06012 reference sample.

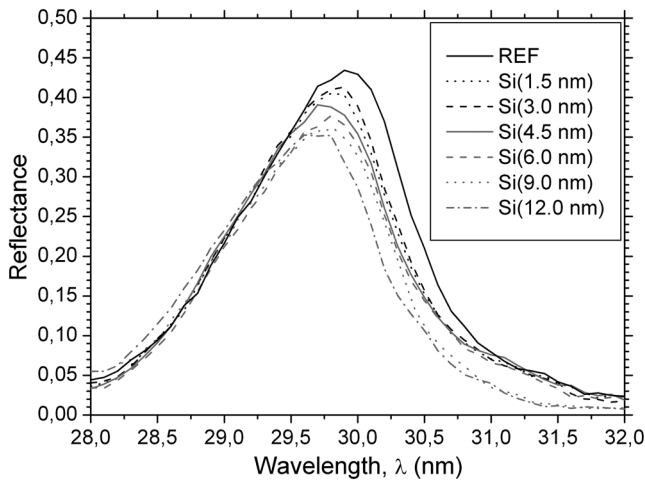


Fig. 5 Reflectance of the samples with additional Si top layer and same structure as the A06012 reference sample.

3 Experimental Characterization and Discussion

After deposition, all samples were characterized in the three spectral bands mentioned above. The reflectances in the EUV band were measured at the NSLS beamline X24C.

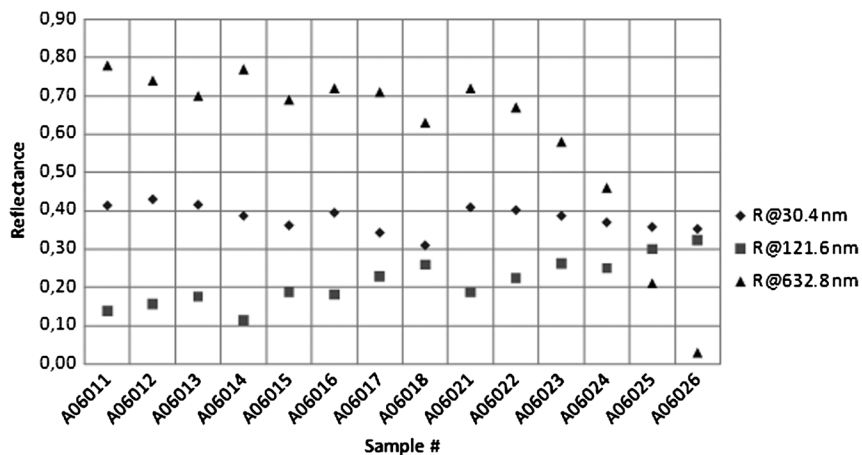


Fig. 6 Experimental reflectance obtained in the EUV region (peak reflectance around 30.4 nm), 121.6 nm, and 632.8 nm for each sample.

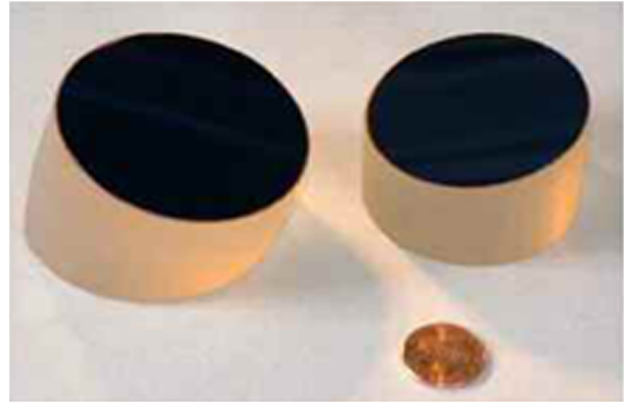


Fig. 7 SCORE flight mirrors.

Reflectances in the visible domain were also measured at NSLS. The reflectance measurements at 121.6 nm were also repeated at CNR-IFN LUXOR (Padova, Italy) using a normal incidence reflectometer (see below). The results obtained in the latter facility are completely in agreement with those measured at NSLS. The experimental results were fitted by using the IMD program²⁰ in order to estimate the structural parameters of the coating as deposited. The fitting parameters are reported in Table 3. The formation of a thin oxidized layer was taken into account for both the Si and SiC top layer, as suggested by Presser and Nickel.²¹ The experimental results are shown in Figs. 3, 4, and 5.

The structural parameters derived from the fits are different from those theoretically defined during design optimization. In particular, variation of about 20% can be detected both in Γ and d values with respect to the nominal ones. These errors can be attributed both to errors in deposition layer thickness and/or to the fitting procedure. In fact, the fitting is obtained with a multilayer model usually adopted, in which the variable parameters are the layer thicknesses and the roughness at the interfaces, while the optical constants are those available in the CXRO database, and the presence of compounds which may form at the multilayer interfaces is neglected. Considering that the layer thicknesses were very well controlled during deposition, the mismatch between theoretical gamma and experimental data can be attributed to the limitation of the fitting more than to experimental deposition error. In Fig. 6, experimental results

Table 4 The EUV peak reflectance obtained a few weeks after deposition and after four years of aging.

CODE	Peak <i>R</i> before	Peak <i>R</i> after
A06012	0.43	0.30
A06011	0.42	NA
A06013	0.42	0.31
A06014	0.39	NA
A06012	0.43	0.30
A06015	0.37	0.36
A06016	0.40	0.38
A06017	0.35	0.34
A06012	0.43	0.29
A06021	0.41	0.31
A06022	0.40	0.06
A06023	0.39	0.02
A06024	0.38	NA

obtained in the EUV range, at 121.6 and 632.8 nm, respectively, are summarized for each sample.

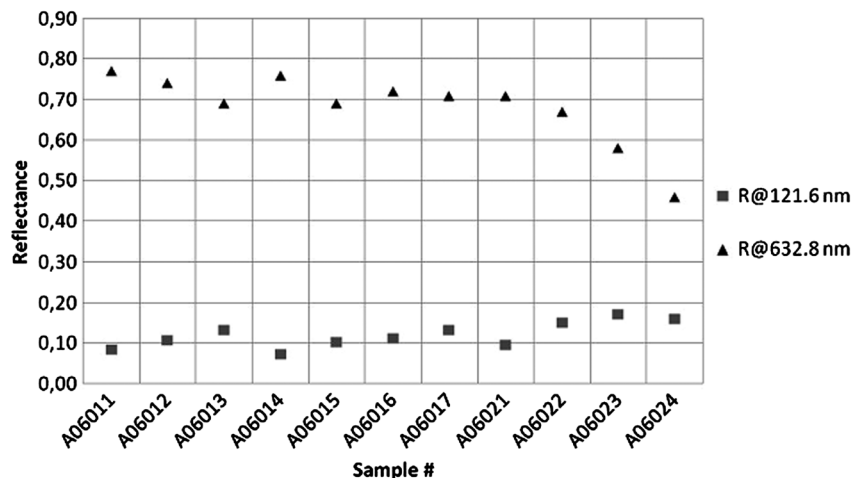
The best choice for the SCORE application appeared to be sample A06026, because it presents the highest efficiency at the H I Lyman- α line without compromising the performances at 30.4 nm, and the flight mirrors were coated with this same structure (Fig. 7).

The laboratory samples were stored for years in plastic boxes kept under regular atmosphere. The reflectance characterizations at 121.6 nm and in the visible spectral range were repeated for selected samples (listed in Table 4) after 3.5 years after deposition. In order to perform these measurements, the samples were handled under regular atmosphere. The sample corresponding to the mirror coating (A06026) used for the SCORE flight was no longer avail-

able, due to its utilization in the post-launch characterization experiment of the SCORE telescope. For the purposes of the present work, we thus measured the reflectance of all the remaining samples. The reflectance at 121.6 nm was measured again using the normal incidence reflectometer at CNR-IFN LUXOR. The setup used in the experiment consists of an Hamamatsu deuterium lamp coupled with a monochromator mounted in Johnson-Onaka configuration. A toroidal mirror focuses the beam exiting from the monochromator in the test chamber equipped in $\theta-2\theta$ configuration. The measurements were performed at 121.6 nm for different incidence angles in two orientations of the test chamber rotated 90 deg with respect to one another. The results of the two measurements were then averaged to obtain the reflectance in the case of unpolarized light. Incident and reflected beam intensity were acquired by a channel electron multiplier (CEM) detector in photon counting mode, and the reflectance curves were recovered using the ratio between the two signals. Reflectance in the visible spectral range was measured using a double grating spectrophotometer (Varian model, Cary 5000). Both regular (at 8 deg incidence angle) and diffuse data were obtained by using an integrating sphere accessory.

A 30% degradation was observed at 121.6 nm in all remeasured samples. No degradation was observed in the visible spectral region at this time, the diffuse component being negligible with respect to the regular reflected light. At the same time, by visual inspection, the surface starts to present some inhomogeneities. The experimental results after 3.5 years are shown in Fig. 8 for the 121.6 nm and visible range.

After five additional months, the selected samples of Table 4 were retested at the ELETTRA BEAR beamline²² to verify their stability in terms of EUV efficiency. Some of the samples showed stable peak values, while other samples were significantly degraded compared to performance measured just after deposition. In Fig. 9, reflectance curves of samples that show partial or no degradation are reported, while those that show strong degradation are not reported. Furthermore, in some cases, the reflectance in the visible spectral range was so low that sample alignment in the BEAR beamline experimental chamber was not feasible, preventing the possibility to test them. (Reflectance of these samples is noted as NA in Table 4) In fact, the appearance of the coatings

**Fig. 8** Experimental reflectance retested after 3.5 years at 121.6 nm and 632.8 nm for each sample.

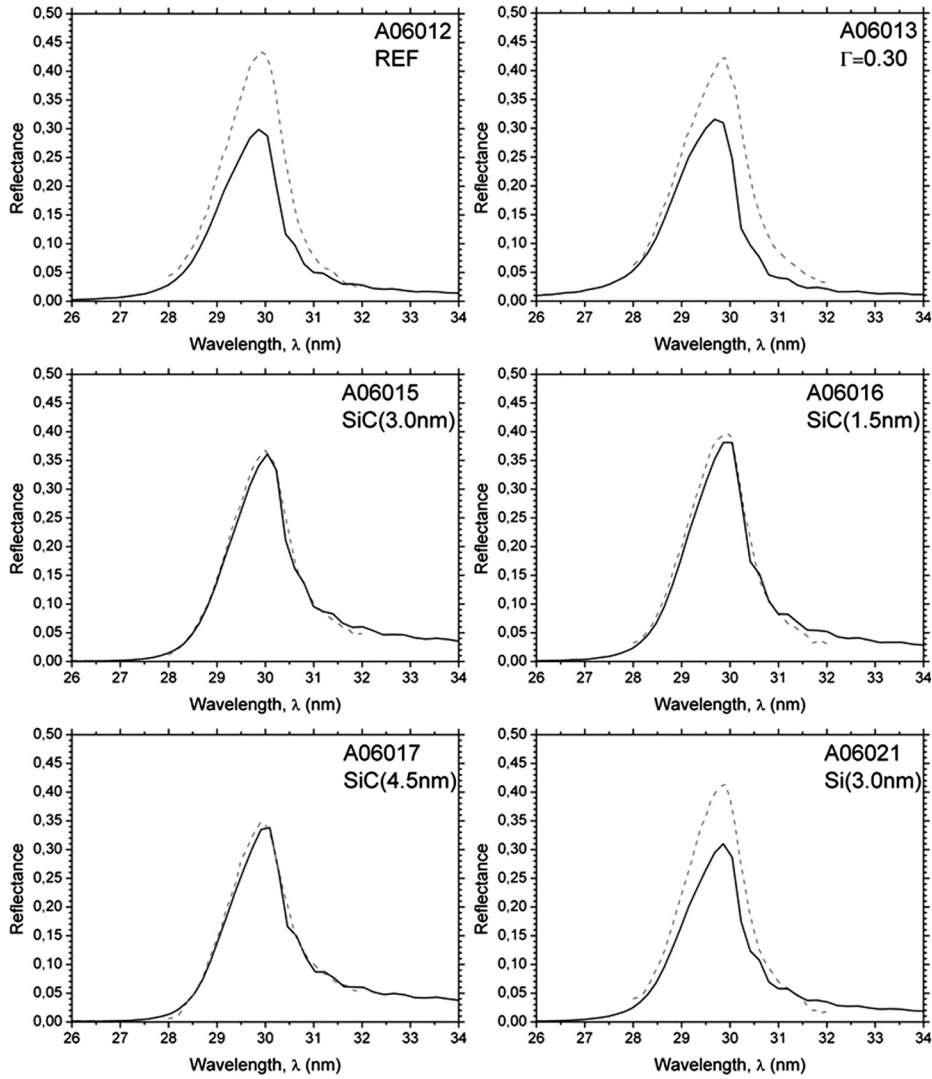


Fig. 9 Comparison between EUV reflectance measured a few weeks after deposition (dashed line) and four years after deposition (continuous line).

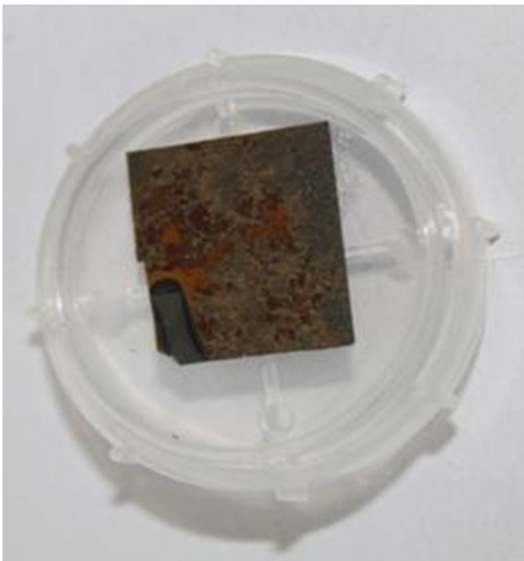


Fig. 10 Appearance of SiC/Mg multilayer samples four years after deposition and exposure to regular atmosphere.

Table 5 EUV percentage reflectance loss and AFM roughness on sample surface.

CODE	$\% \Delta R/R$	σ RMS	Σ PV
A06012	30%	6 nm (A)/ 12 nm (B)	0.8-30 nm (A)/ 38-70 nm (B)
A06011	NA	13 nm	17-87 nm
A06013	26%	5 nm	8-20 nm
A06014	NA	23 nm	28-280 nm
A06016	5%	2 nm	0.3-3 nm
A06017	2%	1 nm	0.5-20 nm
A06021	25%	11 nm	0.6-3.8 (A)/ Large undulations (B)
A06022	85%	—	16-65 nm
A06023	95%	—	Large undulation all over the surf.

at this time was further degraded, showing large, inhomogeneous rough areas observable by eye. In Fig. 10, a picture taken five months after the opening of the plastic boxes in which the samples were stored clearly shows a strongly degraded appearance, if compared with the mirrors of Fig. 7. A large corroded area on the surface, probably related to chemical properties of Mg, is present on all samples.

Despite such appearance and top surface degradation, some samples still performed well in the EUV range. The degradation of the performance at 30.4 nm seems instead to be related to the surface structural properties of the samples. First of all, all remeasured Si capped MLs showed strong degradation. Among the MLs having a SiC top layer, those with an additional SiC capping layer can be considered as stable in the EUV region over a period of

four years. If we analyze the samples considering the variation of the Γ , we can see that sample AO6012 partially degrades, samples A06014 and A06011 degrade more compared to the reference, and sample A06013 degrades less than the reference. This behavior can be directly related to the Mg layer thickness: samples with thicker Mg layers degrade to a larger degree after four years.

4 Atomic Force Microscopy Characterization

The morphology of the selected samples was characterized by using the Atomic Force Microscope (AFM) operating in noncontact mode (XE-70, Park System). In Table 5, the percentage of reflectance loss measured four years after deposition is reported for the samples analyzed, together

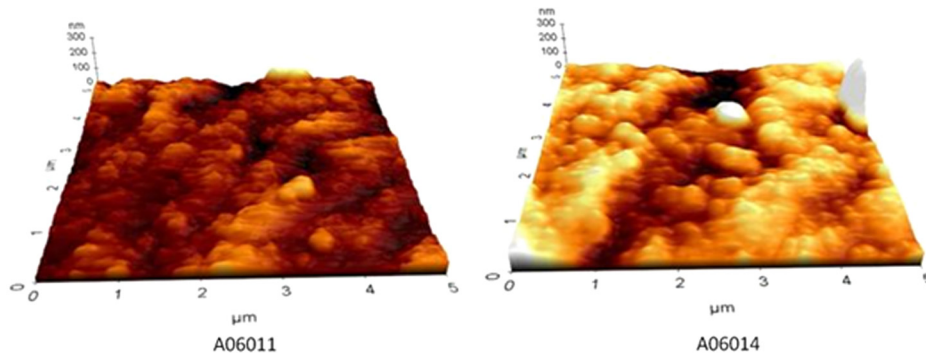


Fig. 11 AFM of samples with modified Γ .

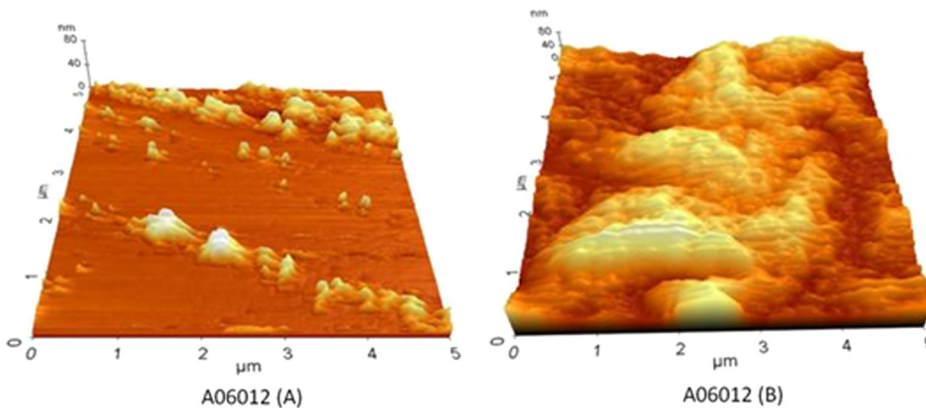


Fig. 12 AFM of reference sample A06012.

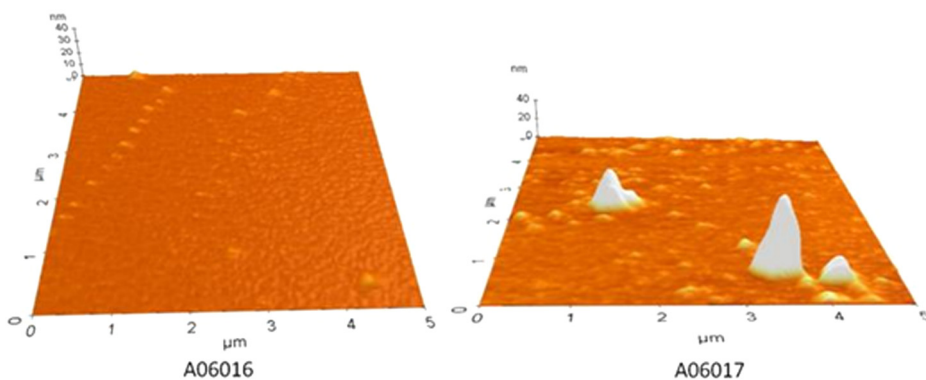


Fig. 13 AFM of samples with an additional SiC top layer.

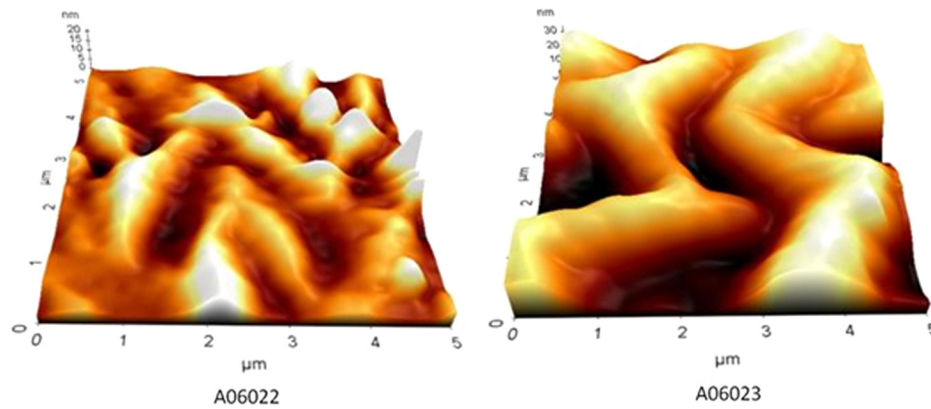


Fig. 14 AFM of samples with an additional Si top layer.

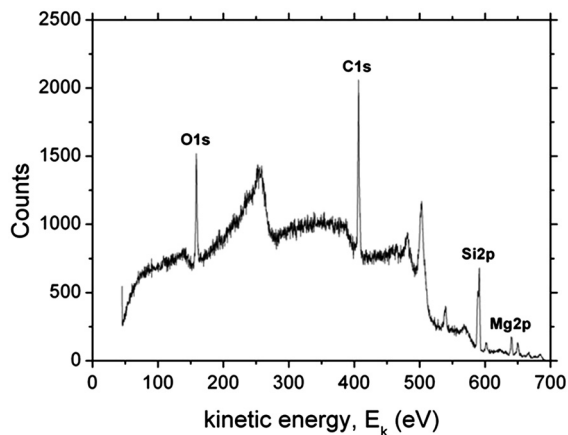


Fig. 15 XPS survey spectrum of the sample A06011, which shows the presence of Mg on the top layer. The identification of atomic species was done with reference to Au 4f peaks.

with the related micro-roughness and the maximum and minimum Peak-Valley (PV) values calculated over a $5 \times 5 \mu\text{m}^2$ area. Since, in some samples, the morphology changes significantly over the top surface, areas with different characteristics were considered. Therefore, two values are given both for micro-roughness and PV.

Analyzing the samples which have a Γ identical to that of the A06012 reference, those that do not reflect any longer after 4.5 years have higher roughness than those that still partially perform. The AFM images of the surfaces of the samples, as for instance A06011 and A06014 (Fig. 11), show “bubbles” everywhere, whereas sample A06012 displays some areas with the same “bubble” appearance (B) and some others that present a lower roughness value (A) (Fig. 12). The associated roughness and PVs are higher for those samples that have higher reflectance loss. In the case of samples with a SiC additional top layer (Fig. 13), the morphology of the surface remains more regular and smooth, even though it is possible to suppose that a process similar to that in A06012(B) is ongoing, and further degradation will probably be observed in time. Finally, in Fig. 14, an AFM image of samples with Si on top is reported (A06022 and A06023). In this case, the morphology presents some low frequency undulations that completely alter the mirror properties of the sample. Sample A06021 has some areas which are characterized by the same effect (B), while

some others are not yet affected by such undulations. This scenario, determined by the qualitative analysis carried on as described, indicates that, in this case, the degradation also is ongoing, and thus further degradation is expected. The physical processes progressing on the surfaces are compatible with a strong degradation of the interfaces, large inter-diffusion of Mg in SiC, and, at the top surface, oxidation of Mg itself.

X-ray Photoemission Spectroscopy (XPS) was carried out on samples A06012, A06011, and A06016 at the BEAR beamline of ELETTRA. In particular, the XPS survey photons (energy 700 eV, pass energy 20 eV, binding energy step 0.304 eV) confirm that Mg is present on the top layer of the samples (Fig. 15). A preliminary analysis of the XPS data shows that the amount of Mg is related to the degradation of the reflectance.

5 Conclusion

Different Mg/SiC ML samples were fabricated on Si wafer substrates varying the structural parameters and/or the capping layer material and its thickness. They were characterized in the EUV range, at 121.6 nm, and in the visible spectral range a few weeks after deposition. Their performance was verified years after deposition, a period during which the samples were initially stored in a sealed plastic box (3.5 years) and then in boxes exposed to regular atmosphere (five additional months). After four years, samples show a large surface modification, probably due to Mg corrosion, which affects their reflectance in the visible spectral range and at 121.6 nm. Nevertheless, the performance in the EUV is not related to the degraded surface characteristics, since some samples still perform well, despite the observed alteration. The degree of degradation is likely to be related to the structural parameters of the multilayer and the characteristics of the capping layer. In particular, all the samples with a Si top layer underwent a complete degradation, samples with a SiC top layer deposited over the last SiC layer exhibit unaltered performances, and samples with modified Γ ratios show partial degradation, which can be associated with the thickness of Mg in the bilayers. A detailed AFM analysis shows that the physical process responsible for degradation is present in all samples at different evolution stages, and thus further reflectance reductions have to be expected in those samples which are degrading more slowly. The processes occurring on the surface are compatible with a large

interdiffusion at the Mg/SiC interfaces and, at the top surface, oxidation of Mg itself. This fact has been confirmed by XPS analysis, which revealed the presence of Mg in the top layers. A potential solution to slow down this process might consist in increasing the SiC top layer thickness for protection, or adding a barrier layer between the SiC and the first two Mg layers.

Acknowledgments

The authors thank Prof. Ester Antonucci, INAF-OATO, Principal Investigator of METIS (Solar Orbiter) and SCORE, and Dr. A. Giglia for measurement at BEAR beamline. This work has been performed with the financial support of the Italian Space Agency (ASI/INAF/015/07/0 and ASI/INAF/Solar Orbiter) and of the Cassa di Risparmio di Padova e Rovigo (CARIPARO) Foundation—Bandi di Eccellenza 2009/2010. The author thanks EU COST Action MP0601 “Short wavelength laboratory sources”.

References

- G. Naletto et al., “METIS, the multielement telescope for imaging and spectroscopy for the solar orbiter mission,” *Proc. ICSO—International Conference on Space Optics*, Rhodes, Greece (October 4–8 2010).
- “Solar orbiter exploring the sun-heliosphere connection,” *Assessment Study Report ESA/SRE* (2009).
- S. Fineschi, “Inverted-COR: inverted-occultation coronagraph for solar orbiter,” *Technical Report INAF-Osservatorio Astronomico di Torino*, **119** (2009).
- S. Fineschi, “Spectra-COR: spectral capability for the inverted-COR on solar orbiter,” *Technical Report INAF-Osservatorio Astronomico di Torino*, **120** (2009).
- J. P. Delaboudineire et al., “EIT: extreme-ultraviolet imaging telescope for the SOHO mission,” *Sol. Phys.* **162**(1–2), 291–312 (1996).
- D. Berghmans et al., “SWAP on board PROBA 2, a new EUV imager for solar monitoring,” *Adv. Space Res.* **38**(8), 1807–1811 (2006).
- S. Bajt et al., “Improved reflectance and stability of Mo/Si multilayers,” *Opt. Eng.* **41**(08), 1797–1804 (2002).
- V. Rigato et al., “Effects of ion bombardment and gas incorporation on the properties of Mo/a-Si : H multilayers for EUV applications,” *Surf. Coat. Tech.* **174**, 40–48 (2003).
- A. J. Corso et al., “Capped Mo/Si multilayers with improved performance at 30.4 nm for future solar missions,” *Opt. Express* **19**(15), 13963–13973 (2011).
- M. G. Pelizzo et al., “High performance euv multilayer structures insensitive to capping layer optical parameters,” *Opt. Express* **16**(19), 15228–15237 (2008).
- M. Suman et al., “Aperiodic multilayers with enhanced reflectivity for extreme ultraviolet lithography,” *Appl. Opt.* **47**(16), 2906–2914 (2008).
- P. Zuppella et al., “Iridium/silicon multilayers for EUV applications in the 20–35 nm wavelength range,” *Opt. Lett.* **36**(7), 1203–1205 (2011).
- M. H. Hu et al., “Structural properties of Al/Mo/SiC multilayers with high reflectivity for extreme ultraviolet light,” *Opt. Express* **19**(18), 20019–20028 (2010).
- R. Soufli et al., “Development and testing of EUV multilayer coatings for the atmospheric imaging assembly aboard the solar dynamics observatory,” *Proc. SPIE* **5901**, 59010M-1 (2005).
- J. T. Zhu et al., “Comparison of Mg-based multilayers for He II radiation at 30.4 nm wavelength,” *Appl. Optics* **49**(20), 3922–3925 (2010).
- H. Takenaka et al., “Soft-X-ray reflectivity and heat resistance of SiC/Mg multilayer,” *J. Electron Spec. and Rel. Phen.* **144**, 1047–1049 (2010).
- M. G. Pelizzo et al., “Design, deposition, and characterization of multilayer coatings for the ultraviolet and visible-light coronagraphic imager,” *Appl. Optics* **43**(13), 2661–2669 (2004).
- S. Fineschi et al., “Ultraviolet and visible-light coronagraphic imager (UVCI) for HERSCHEL (helium resonance scattering in corona & heliosphere),” *SPIE* **4853**, 162–171 (2003).
- D. L. Windt and W. K. Waskiewicz, “Multilayer facilities for EUV lithography,” *J. Vac. Sci. Technol. B* **12**(6), 3826–3832 (1994).
- D. L. Windt, “IMD: Software for modelling the optical properties of multilayer films,” *Comput. Phys.* **12**(4), 360–370 (1998).
- V. Presser and K. G. Nickel, “Silica on silicon carbide,” *Crit. Rev. Solid State* **33**(1), 1–99 (2008).
- G. Naletto et al., “The monochromator radiation beamline X-MOSS at ELETTRA,” *SPIE Proc.* **4145**, 105–113 (2001).

Maria Guglielmina Pelizzo graduated in physics from the University of Padua in 1996. She received her PhD in space science and technology in 2001. She is a researcher at the National Research Council of Italy-Institute for Photonics and Nanotechnology (CNR-IFN) and an adjunct professor in the faculty of engineering at the University of Padua. Her research interests are the development and characterization of optical coating and instrumentation for space and physics matter application.

Silvano Fineschi has more than 20 years of experience in the development and operation of space instrumentation for spectroscopy and polarimetry in the visible and ultraviolet wavelength bands. His scientific interests include the application of atomic spectroscopy and polarimetry to UV and visible-light remote-sensing techniques for the study of the solar wind and the coronal magnetic field. He has been involved in several solar space missions (SMM, Spartan/Space-Shuttle, SOHO, Solar Orbiter), sounding-rocket solar experiments, and eclipse campaigns. He is currently the Project Scientist for the METIS coronagraph on the Solar Orbiter mission.

Alain Jody Corso graduated in electrical engineering from the University of Padua in 2010 and is currently a PhD student there. His research interests are the development and characterization of thin films for extreme ultraviolet application and photolithography.

Paola Zuppella earned her PhD in physics from L’Aquila University in May 2009. She is currently a researcher at the National Research Council of Italy-Institute for Photonics and Nanotechnology (CNR-IFN). Her research interests are the development and calibration of optical instrumentation for space and physics matter application.

Biographies of the other authors not available.